

Chemical Property Prediction Under Experimental Biases

Yang Liu and Hisashi Kashima

Department of Intelligence Science and Technology, Kyoto University

Abstract. The ability to predict the chemical properties of compounds is crucial in discovering novel materials and drugs with specific desired characteristics. Recent significant advances in machine learning technologies have enabled automatic predictive modeling from past experimental data reported in the literature. However, these datasets are often biased due to various reasons, such as experimental plans and publication decisions, and the prediction models trained using such biased datasets often suffer from over-fitting to the biased distributions and perform poorly on subsequent uses. The present study focuses on mitigating bias in the experimental datasets. To this purpose, we adopt two techniques from causal inference and domain adaptation combined with graph neural networks capable of handling molecular structures. The experimental results in four possible bias scenarios show that the inverse propensity scoring-based method makes solid improvements, while the domain-invariant representation learning approach fails.

1 Introduction

The ability to predict the chemical properties of compounds is crucial in discovering novel materials and drugs with specific desired characteristics. To accelerate the discovery process, a variety of computational approaches, including those based on density functional theory, have been widely used; however, they are still expensive and time-consuming. In recent decades, researchers have turned to data-driven approaches using fast-progressing machine learning technologies [31]. This trend has been further accelerated by the remarkable development of deep learning in recent years; in particular, graph neural networks (GNNs) have achieved remarkable performance in predicting chemical properties via automatic feature extraction from molecular structures represented as graphs [6,9]. Their applications have expanded to a variety of tasks, such as molecular generation [23,46,5], molecular explanation [45,2], and analysis of intermolecular interactions [14,39].

The construction of accurate predictive models often relies on large-scale labeled data sets; they are usually collections of knowledge, such as experimental results reported on scientific papers, that are the product of tremendous scientific efforts. Unsurprisingly, scientists do not sample molecules from a vast chemical space uniformly at random nor based on their natural distribution; rather, their decisions on experimental plans or publication of results are biased

by physical, economic, or scientific reasons. For instance, a large proportion of molecules are not investigated experimentally due to factors related to molecular mechanics, such as solubility [24], weights [29], toxicity [13] and side effects, or factors related to molecular structure such as crystals [17]. Concerns about the cost and availability of molecules can also be reasons to exclude certain groups of molecules. Conversely, popularity considerations based on current research trends [15] and the experimental methods in which each lab specializes [37] drive the selection of compounds. These propensities related to the researchers’ experience and knowledge can contribute to more efficient search and discovery in the chemical space, but on the other hand, they influence the data in an undesirable way. Prediction models trained using such biased datasets often suffer from over-fitting to the biased distributions, which leads to poor performance on subsequent uses [18,38,3].

Despite the reported evidence on the existence of bias in scientific experiments and their harmful effects, almost no attempts to address this issue have been reported. In this study, we focus on mitigating the sources of bias in the experimental datasets by applying two techniques from causal inference and domain adaptation, i.e., inverse propensity scoring (IPS) [16,32] and domain-invariant representation learning (DIRL) [8,33,43]. In the IPS approach, we first estimate the propensity score function, which represents the probability of each molecule to be analysed, and then estimate the chemical property prediction model by weighting the objective function with the inverse of the propensity score. The DIRL approach is based on more recent advancements of representation learning of deep neural networks for transfer learning and causal inference. It consists of a feature extractor, a domain classifier, and a label predictor, where the feature extractor extracts features that help the label predictor while discouraging the domain classifier, and the whole network is optimized in an end-to-end manner. Both approaches are implemented over a GNN to handle the molecular structures of the compounds.

In the experiments, we use the well-known large-scale dataset QM9, consisting of exhaustively enumerated small-molecule structures associated with 12 fundamental chemical properties. Because it is impossible to know how a publicly available dataset is truly affected by bias, we simulate four practical biased sampling scenarios from the dataset, which introduce significant biases in the observed molecules. Under each biased sampling scenario, we validate our proposed models for predicting 12 chemical properties as 12 regression problems. The experimental results show that the IPS approach improves the predictive performance in all the scenarios on most of the targets with statistical significance compared with the baseline. On the other hand, contrary to our expectations, the (more modern) DIRL approach reduces predictive performance in all of the bias scenarios. This is probably because the information that is useful for the domain classifier is also useful for predicting chemical properties, and is eliminated by the DIRL approach. These results provide useful insights for future developments of the proposed methods.

In summary, the main contributions of this work are as follows:

- We first address the problem of predicting properties of chemical compounds under experimental biases.
- We introduce two bias mitigation techniques, IPS and DIRL, combined with graph neural network-based chemical property prediction.
- We validate the two proposed approaches under various experimentally biased sampling scenarios, and show IPS improves the prediction performance, whereas DIRL worsens it.

2 Problem Setting

Let us assume that we are given a training dataset $\mathcal{D}^{\text{train}} = \{(G_i, y_i)\}_{i=1}^N$ including N molecular graphs, where $G_i \in \mathcal{G}$ is a molecular graph (biasedly) sampled from the universe of molecules \mathcal{G} , and $y_i \in \mathbb{R}$ is the target chemical property. Each molecular graph $G_i = (\mathcal{V}_i, \mathcal{E}_i, \sigma_i) \in \mathcal{G}$ has a set of nodes (i.e., atoms) \mathcal{V}_i , a set of edges (i.e., bonds) $\mathcal{E}_i \subseteq \mathcal{V}_i \times \mathcal{V}_i$, and a label function $\sigma : \mathcal{V}_i \cup \mathcal{E}_i \rightarrow \mathcal{L}$, where \mathcal{L} is the set of possible node labels (i.e., atom types such as hydrogen and oxygen) and edge labels (i.e., bond types such as double bond and aromatic bond).

Our goal is to obtain a prediction function $f : \mathcal{G} \rightarrow \mathbb{R}$ that predicts a particular target chemical property over the molecule universe \mathcal{G} that we are interested in. We assume we have a uniformly randomly sampled part of (or possibly the whole) chemical universe, consisting of M molecules $\mathcal{D}^{\text{test}} = \{G_i\}_{i=N+1}^{N+M}$.

The main difficulty in this problem is that the training data is constructed from past experiments reported in the literature, and therefore is significantly biased with respect to the uniform distribution over the chemical universe due to decisions taken by the researchers on experimental plans or publication options. There is no guarantee that the predictor derived from the biased training data has high predictive performance even on the chemical universe.

Note that the $\mathcal{D}^{\text{test}}$ can also be a biased sample; however, without loss of generality, we just assume it is a uniformly random subset of the molecules we are interested in.

3 Methods

We start with reviewing the GNN architecture that is the fundamental building block of our model, and then describe two bias canceling schemes, inverse propensity scoring (IPS) and domain-invariant representation learning (DIRL); they are combined to tackle the problem of chemical graph property prediction under experimental biases.

3.1 Graph neural networks for chemical property prediction

Among many successful graph neural networks, we choose the message-passing GNN architecture proposed by Gilmer et al. [9] for its generality, simplicity, and fair performance in the chemical domain.

A GNN takes a graph $G = (\mathcal{V}, \mathcal{E}, \sigma) \in \mathcal{G}$ as its input. In the t -th layer of the GNN, it updates the current set of the node representation vectors $\{\mathbf{h}_v^t\}_{v \in \mathcal{V}_i}$ to $\{\mathbf{h}_v^{t+1}\}_{v \in \mathcal{V}_i}$. Specifically, the representation vector of node v is updated depending on the current vectors of its neighbor nodes using the update formula

$$\begin{aligned} \mathbf{m}_v^{t+1} &= a \left(\sum_{u \in \mathcal{N}(v)} m_t(\mathbf{h}_v^t, \mathbf{h}_u^t, \sigma(v, u)) \right), \\ \mathbf{h}_v^{t+1} &= u_t(\mathbf{h}_v^t, \mathbf{m}_v^{t+1}), \end{aligned} \quad (1)$$

where $\mathcal{N}(v)$ denotes the set of the neighbor nodes of v , while m_t is a so-called message passing function that collects the information (i.e., the representation vectors) of the neighbors, that is a linear function of $(\mathbf{h}_v^t, \mathbf{h}_u^t)$ depending on the edge label $\sigma(v, u)$. The a is an activation function, for which we choose the rectified linear unit (ReLU) function. The u_t is the vertex update function, for which we use the gated recurrent unit (GRU). The initial node representations $\{\mathbf{h}_v^0\}_{v \in \mathcal{V}}$ are initialized depending on their atom types. As the message passing operation is repeatedly applied, the node representation vector gradually incorporates information about its surrounding structure.

After being processed through T layers, the final node representations $\{\mathbf{h}_v^T\}_{v \in \mathcal{V}}$ are obtained; they are aggregated to the graph-level representation \mathbf{h}_G using a readout function r , that is,

$$\mathbf{h}_G = r(\{\mathbf{h}_v^T\}_{v \in \mathcal{V}}), \quad (2)$$

where we could simply use summation followed by a linear transformation as the readout function. However, in our implementation, we use a slightly more complex solution, i.e., an LSTM pooling layer followed by a linear layer.

The graph-level representation \mathbf{h}_G is passed to the final layer to give the outputs of the GNN, such as the chemical property prediction, the propensity score, and the domain classification, as we will see later.

3.2 Bias correction using inverse propensity scoring (IPS)

If we assume there are no biases in our training dataset, the distributions of the training dataset and the target (test) dataset are identical. This means that minimizing the empirical mean of the loss function ℓ , that is,

$$\frac{1}{N} \sum_{i=1}^N \ell(y_i, f(G_i)), \quad (3)$$

directly leads to obtaining a good prediction model that achieves a small expected loss $E[\ell(y, g(G))]$ for the test data. However, in our situation where the training dataset is sampled in a biased manner, the minimization of the standard empirical loss results in a biased prediction model.

One of the possible remedies to this problem is the use of a propensity score [16] to adjust the importance weight of each training instance. The propensity score $\pi(G)$ of molecular graph G is the probability that the molecule is included in the experimental data. The loss for each molecule is inversely weighted with the propensity score, which results in the modified objective function:

$$o^{\text{IPS}}(f) = \frac{1}{N} \sum_{i=1}^N \frac{1}{\pi(G_i)} \ell(y_i, f(G_i)). \quad (4)$$

With the correct propensity score function π , the weighted loss function is unbiased with respect to the uniform sampling from the molecular universe.

The IPS approach consists of two steps: propensity score estimation and chemical property prediction. We first estimate the propensity score function representing the probability of each molecule being experimented. It is estimated from the biased training dataset and the unbiased test set (uniformly sampled from the molecule universe). This step is usually performed by solving a two-class probabilistic classification problem to classify the two datasets using the logistic loss (a.k.a. the cross entropy loss). Note that the target property values are not used for propensity modeling.

The second step estimates the chemical property prediction model with the loss function weighted using the inverse of the propensity score. We use the squared loss function as ℓ , and the problem is cast as a weighted regression problem.

The propensity score function and the chemical property prediction model are both implemented as GNNs because they take graph-structured molecules as their inputs.

3.3 Bias correction using domain-invariant representation learning (DIRL)

The domain-invariant representation learning approach [8,33,43] is another option to correct sample selection biases. We adopt the best-known method proposed by Ganin et al. [8], which we refer to as DIRL. It requires three components: a feature extractor, a domain classifier, and a label predictor, denoted by f_F , f_D , and f_L , respectively. In contrast with IPS that has two separate GNN models, there are two paths from the input (i.e., a molecular graph) to two outputs in one single model; the first path is to make chemical property predictions, and is specified by a label predictor f_L concatenated after a feature extractor f_F . The second path is for domain classification, which is specified by a domain classifier f_D concatenated after the feature extractor f_F . Note that f_F commonly appears in both of the paths. The final deliverable f that we want is the composite function of f_F and f_L , that is, $f(G) = f_L(f_F(G))$. The domain classifier itself is not directly what we actually want for our final goal, but it helps to extract de-biased representations of the inputs in the training phase.

In the training phase, the first path (consisting of f_F and f_L) aims to predict the target chemical property, by minimizing

$$o^{\text{property}}(f_F, f_L) = \frac{1}{N} \sum_{i=1}^N \ell(y_i, f_L(f_F(G_i))), \quad (5)$$

where ℓ is the loss function for chemical properties, namely, the squared loss in our case. In the second path (including f_F and f_D), the domain classifier f_D aims to correctly classify the domain (i.e., training or test) of the input, while the feature extractor f_F aims to prevent the correct classification. Therefore, denoting by c the loss function for domain classification (that is, the logistic loss in our case), the objective function for the second path is given as

$$o^{\text{domain}}(f_F, f_D) = \frac{1}{N+M} \sum_{i=1}^{N+M} c(d_i, f_D(f_F(G_i))), \quad (6)$$

where d_i indicates the domain that G_i belongs to (i.e., training or test). Note that f_D tries to minimize this objective function, while f_F tries to maximize it. The overlap between the minimization and the min-max problem is actually an undesirable feature in the process of solving the optimization problem; especially for the feature extractor aiming to minimize o^{property} and maximize o^{domain} . To handle this situation simply with back-propagation, a special layer called gradient reversal layer is often used. The gradient reversal layer denoted by r is an identity function $r(\mathbf{x}) = \mathbf{x}$ in forward calculations, but the derivative is defined as $\frac{\partial r}{\partial \mathbf{x}} = -\mathbf{I}$. With the gradient reversal layer, the second objective function o^{domain} is rewritten as

$$o^{\text{domain}}(f_F, f_D) = \frac{1}{N+M} \sum_{i=1}^{N+M} c(d_i, f_D(r(f_F(G_i)))) \quad (7)$$

so that the whole optimization problem becomes a pure minimization problem.

Since we optimize the whole network at once, the overall objective function is the sum of o^{property} and o^{domain} ,

$$o^{\text{DIRL}}(f_F, f_D, f_L) = o^{\text{property}}(f_F, f_L) + o^{\text{domain}}(f_F, f_D). \quad (8)$$

4 Experiments

4.1 Biased sampling scenarios

Chemists consciously or unconsciously select the molecules to be used in their experiments, depending on a variety of factors such as molecular structure, properties, cost, and popularity. Since we cannot know why the compounds reported in the literature were selected, we simulate several possible scenarios for sampling our training datasets.

In our experiments, we consider the following four possible biased sampling scenarios:

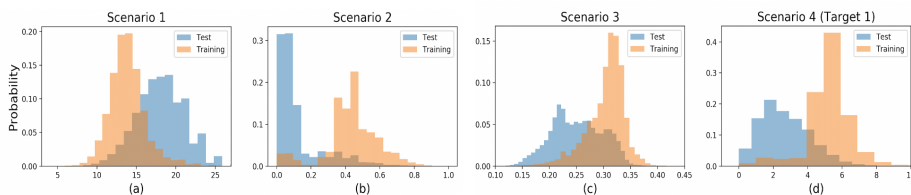


Fig. 1. Average densities of the training dataset and the test dataset. The x -axes correspond to (a) number of atoms, (b) proportion of double/triple/aromatic bonds, (c) value of HOMO-LUMO Gap (gap), and (d) value of μ , respectively.

Scenario 1 assumes molecules with a smaller number of atoms have higher sampling chances, because smaller molecules are thought to be more common and better-studied [22]. In the QM9 dataset, the number of atoms ranges from 3 to 27.

Scenario 2 prefers molecules with smaller proportions of single bonds (i.e., with higher proportions of the other bond types). The spectral manifestations of chemical functional groups greatly depend on bond types within the group [34]. For simplicity, we assume that less single-bonded molecule would have stronger spectral manifestations.

Scenario 3 selects molecules with higher values of the HOMO-LUMO Gap, because larger HOMO-LUMO Gap values often indicate higher stability and lower chemical reactivity [1].

Scenario 4 assumes scientists focus on compounds with high target property values based on their expertise and experience to conduct experiments. Compounds with higher targets values have higher sampling chances.

4.2 Datasets

We use the chemical molecule dataset QM9 [28] as the universe \mathcal{G} of the small graphs. QM9 is a publicly available dataset covering 134,000 small stable organic molecules made up of hydrogen (H), carbon (C), oxygen (O), nitrogen (N), and fluorine (F). They are the subset of all the molecules with up to nine heavy atoms (C, O, N, F) out of the 166 billion molecules of the GDB-17 chemical universe [30,28]; therefore we consider the QM9 dataset as the natural universe of molecules made of C, O, N, and F.

Each molecule in QM9 has 12 fundamental properties [28]: dipole moment (μ), isotropic polarizability (α), highest occupied molecular orbital energy (homo), lowest unoccupied molecular orbital energy (lumo), gap between homo and lumo (gap), electronic spatial extent (r_2), zero point vibrational energy (zpve), internal energy at 0K (u_0), internal energy at 298.15K (u_{298}), enthalpy at 298.15K (h_{298}), free energy at 298.15K (g_{298}), and heat capacity at 298.15K (cv); they are used as 12 targets for 12 regression tasks.

According to each of the four biased sampling scenarios, we sample a biased training dataset with a size of approximately 10% of the whole QM9 dataset (i.e., approximately 13,400 compounds). Each compound has a sampling chance determined by the sigmoid function depending on the corresponding sampling criteria. For example, in Scenario 1, the smallest molecules with three atoms have the largest sampling chances, while the ones with 27 atoms have the smallest chances. The larger the gain of the sigmoid curve becomes, the more the training and test dataset are separated; we tune the gain so that the average sampling probability becomes 10%.

A test dataset of the same size is then sampled uniformly at random from the remaining molecules. We use sampling without replacement, so no graph belongs to the training set and the test set simultaneously.

We repeat the sampling procedure 30 times to build training and test datasets for statistical testing. Figure 1 shows the average densities of the 30 trials under the biased sampling scenarios (for Scenario 4, only the first target among the 12 targets is shown due to the page limitation). Note that the test density of the test dataset reflects that of the whole chemical universe.

4.3 Implementation details

GNN. We use the PyTorch Geometric Library [7] to implement the GNN models that both of our approaches are based on. Each atom is encoded as a 32-dimensional vector depending on the atom type. The message passing function m_t depends on edge types and is 32-dimensional. The update function u_t is a gated recurrent unit with 32 internal dimensions. The readout function r is a sequence-to-sequence layer followed by two linear layers with 32 internal dimensions.

IPS. To apply the IPS approach, we require two GNN models, one for the propensity score function and the other for chemical property prediction. In the former, we use $T = 3$ GNN layers and a logistic function as the final layer because the propensity score gives the probability that a chemical compound is observed. We use the ADAM [20] optimizer with no weight decay and a batch size of 64 for each iteration. We use a learning rate updating scheduler with an initial learning rate of $1e - 5$; this reduces the learning rate by a factor of 0.7 until the validation error stops reducing for five training epochs. The validation datasets are randomly chosen to include 20% of the training set and the test set. The optimized model that achieves the lowest validation error on the validation dataset is applied for inferring the importance.

The chemical property prediction models also has $T = 3$ GNN layers, and the other training settings are almost the same as those for the propensity score model. The validation set is 20% of the training set. Because we have 12 target chemical properties, we train 12 different GNN predictors.

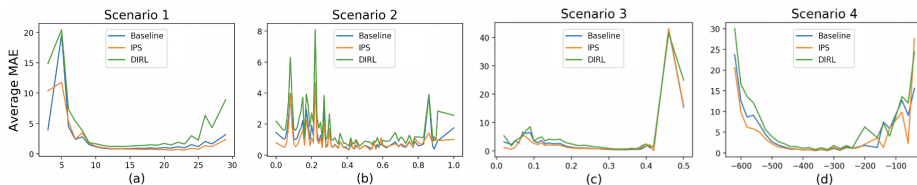


Fig. 2. Average MAE on chemical property u_0 depending on the indicators under four biased sampling scenarios. The x-axes correspond to (a) number of atoms, (b) proportion of double/triple/aromatic bonds, (c) value of HOMO-LUMO Gap (gap), and (d) value of u_0 , respectively.

DIRL. The network structure for the DIRL approach has two output paths: the domain classifier and the label predictor. This structure shares the common feature extraction layers on the input side. We set the number of the GNN layers corresponding to the feature extractor to 3, and those for the domain classifier and the label predictor to 3 and 2, respectively. Similar to the IPS approach, the domain classifier has a readout function for classification (i.e., a logistic function) and the label predictor has one for regression. Note that the feature extractor has no readout function. As is the case with the IPS approach, we use ADAM [20] with no weight decay as the optimizer. We also use a learning rate updating scheduler, with an initial learning rate of $1e-5$, and reduce the learning rate by a factor of 0.7 until the validation error stops reducing for five training epochs. The batch size is set to 64. In contrast with IPS, the whole network is trained in an end-to-end manner. We train 12 DA-GNNs for each of the target properties in each trial. 20% of the training set and the test set are used as the validation set for the domain classifier, and 20% of the training set is used for the label predictor.

Baseline Method. As the baseline method, we use the same GNN structure as the one for IPS, but without bias mitigation. In contrast to the IPS approach, we use the standard average loss for the training dataset (3). The same settings as for IPS are used except for those specific to IPS, such as the number of GNN layers, the choices of the hyperparameters, and the training and validation sets.

Evaluation metrics. The prediction accuracy for each option is evaluated in terms of the average mean absolute error (MAE) obtained from the 30 trials. We also perform the paired t -test to check the statistical significance of performance differences.

4.4 Results

Comparison of predictive performance. We show all the MAE comparison results (in the mean and standard deviations of 30 trials) in Tables 1–4 corresponding to the four simulated biased sampling scenarios. In all four tables, the

Table 1. MAE results under Scenario 1

	Baseline	IPS		DIRL	
mu	0.250±0.016	0.239±0.012	4.5% **	0.287±0.014	-14.5% **
alpha	0.710±0.052	0.649±0.034	8.6% **	0.762±0.043	-7.3% **
homo	0.596±0.019	0.615±0.018	-3.2% **	0.644±0.018	-8.0% **
lumo	0.589±0.028	0.605±0.026	-2.7% *	0.661±0.038	-12.0% **
gap	0.902±0.031	0.935±0.040	-3.6% **	0.944±0.027	-4.6% *
r2	6.357±0.962	6.431±0.945	-1.1%	8.529±0.670	-34.1% **
zpve	0.555±0.035	0.531±0.042	4.4% **	0.958±0.098	-72.5% **
u0	0.947±0.128	0.761±0.094	19.6% **	1.327±0.165	-40.0% **
u298	0.901±0.119	0.687±0.098	23.7% **	1.297±0.106	-44.0% **
h298	0.926±0.116	0.762±0.115	17.6% **	1.473±0.214	-59.1% **
g298	0.890±0.119	0.735±0.120	17.4% **	1.445±0.209	-62.3% **
cv	0.252±0.013	0.228±0.011	9.3% **	0.278±0.014	-10.3% *

Table 2. MAE results under Scenario 2

	Baseline	IPS		DIRL	
mu	0.3405±0.0252	0.3038±0.0212	10.7% **	0.3467±0.0144	-1.8%
alpha	0.8388±0.0864	0.7210±0.0450	14.0% **	0.8729±0.0434	-4.0%
homo	0.7116±0.0268	0.7306±0.0215	-2.6% **	0.7467±0.0377	-4.9% **
lumo	0.7374±0.0562	0.7224±0.0320	2.0%	0.8187±0.0482	-11.0% **
gap	1.1226±0.0510	1.1512±0.0585	-2.5% *	1.1356±0.0423	-1.1%
r2	7.8447±0.6044	8.1287±0.7101	-3.6%	12.310±1.5569	-56.9% **
zpve	0.6459±0.0766	0.5706±0.0523	11.6% **	1.0141±0.1112	-57.0% **
u0	1.1785±0.2493	0.8406±0.2298	28.6% **	1.8660±0.2740	-58.3% **
u298	1.1583±0.2475	0.8741±0.1536	24.5% **	2.1672±0.2963	-87.1% **
h298	1.1266±0.2763	0.8551±0.1932	24.0% **	1.9469±0.4004	-72.8% **
g298	1.2248±0.2712	0.8236±0.1626	32.7% **	2.0564±0.3719	-67.8% **
cv	0.2770±0.0150	0.2468±0.0133	10.9% **	0.3009±0.0168	-8.6% *

ratios in the IPS and DIRL columns indicate the improvements achieved over the baseline, respectively. The ‘*’ symbols next to the improvements denote the p -values reported in the paired t -test; ‘**’ means the p -value is less than 0.01, that is, the increase/decrease is statistically significant with a 1% threshold. Similarly, ‘*’ means that the p -value is less than 0.05, that is, the statistical significance has a 5% threshold.

Table 1 shows the results under Scenario 1, which uses the number of atoms as an indicator for biased sampling. The IPS approach improves the predictive performance with statistical significance compared with the baseline method for eight chemical properties, whereas the DIRL approach degrades the predictive performance for all 12 chemical properties with statistical significance.

Table 3. MAE results under Scenario 3

	Baseline	IPS		DIRL	
mu	0.3067±0.0212	0.3170±0.0267	-3.3%	0.3613±0.0241	-17.8% **
alpha	0.7875±0.0568	0.7748±0.0396	1.6% *	0.9118±0.0413	-15.7% **
homo	0.6748±0.0277	0.6862±0.0288	-1.6%	0.7224±0.0442	-7.0% *
lumo	0.8122±0.0540	0.8064±0.0459	0.7%	0.9459±0.0410	-16.4% **
gap	-	-	-	-	-
r2	6.4950±0.8817	6.3297±0.9999	2.5% *	12.070±1.1736	-85.8% **
zpve	0.6364±0.0760	0.5905±0.0572	7.2% *	0.9601±0.1002	-50.8% **
u0	0.9304±0.1047	0.8305±0.1009	10.7% **	1.6994±0.3591	-82.6% **
u298	0.9857±0.1508	0.8363±0.1068	15.1% **	1.6023±0.2339	-62.5% **
h298	0.9267±0.1001	0.8318±0.1290	10.2% **	1.6712±0.2297	-80.3% **
g298	0.9510±0.1022	0.8645±0.1039	9.0% **	1.6765±0.1783	-76.2% **
cv	0.2410±0.0122	0.2379±0.0101	1.2% *	0.2819±0.0153	-16.9% **

Table 4. MAE results under Scenario 4

	Baseline	IPS		DIRL	
mu	0.4188±0.0450	0.3820±0.0373	8.7% **	0.4231±0.0209	-1.0%
alpha	0.8581±0.0669	0.8412±0.0528	1.9%	0.9452±0.0274	-10.1% *
homo	0.7328±0.0437	0.7274±0.0420	0.7%	0.7789±0.0569	-6.2%
lumo	0.8920±0.0461	0.8943±0.0627	-0.2%	0.9680±0.0672	-8.5% *
gap	1.1090±0.0546	1.1394±0.0588	-2.7% *	1.2268±0.0728	-10.6% **
r2	7.1315±1.0678	6.0009±0.8993	15.8% **	11.092±1.7639	-55.5% **
zpve	0.6573±0.0407	0.6085±0.0586	7.4% **	1.0408±0.0663	-58.3% **
u0	1.0080±0.1510	0.9191±0.1064	8.8% *	1.6332±0.2086	-62.0% **
u298	1.0389±0.1456	0.9226±0.1313	11.1% **	1.6580±0.1620	-59.5% **
h298	1.0300±0.1391	0.9237±0.1162	10.3% **	1.6560±0.2332	-60.7% **
g298	1.0425±0.1304	0.9448±0.1332	9.3% *	1.6450±0.1873	-57.7% **
cv	0.2478±0.0111	0.2527±0.0098	-1.9%	0.2978±0.0176	-20.1% **

Similarly, for Scenario 2, Table 2 shows the statistically significant improvements by IPS for nine chemical properties, and DIRL degrades the predictive performance for nine chemical properties.

Table 3 shows the results under Scenario 3 which uses the HOMO-LUMO Gap value as the indicator for biased sampling, and predicts on 11 other chemical properties. Again, the predictive performance for eight chemical properties is improved with statistical significance by IPS, and DIRL is detrimental to the performance for all 11 chemical properties. Note that the result for the prediction of the HOMO-LUMO Gap is missing in the table (denoted by ‘gap’), but it is equivalent to the result for the HOMO-LUMO Gap in Scenario 4.

Similar results are found in Table 4 corresponding to Scenario 4, where each of 12 chemical properties is used as the indicator for biased sampling in the

prediction tasks for the property itself; IPS improves in eight properties, while DIRL degrades in ten properties.

The overall results for all the scenarios indicate that the IPS approach improves the performance for many properties and scenarios; especially, it is noteworthy that the performance is statistically significantly improved for the six properties (alpha, zvpe, u0, u298, h298, and g298) in all of the four scenarios, which shows that IPS has solid effectiveness and promise in mitigating experimental biases. On the other hand, the DIRL approach is almost harmful for all the scenarios.

The improvements by IPS are more significant for Scenarios 1 and 2 than Scenarios 3 and 4. The differences might be explained by the accuracy of the propensity score model; the accuracies in the four scenarios are 81.05%, 87.49%, 76.04%, and 79.02%, respectively, which mean that the propensity scores are more accurate in Scenarios 1 and 2.

Prediction accuracy depending on indicators for biased sampling. We further investigate why the IPS approach successfully corrects the bias while the DIRL approach fails, by visualizing the prediction accuracy depending on the indicators used in the biased sampling scenarios.

Due to space limitations, we only show the predictive performance for the chemical property u0 in Figure 2. The horizontal axes in the figure correspond to the indicators, namely, (a) the number of atoms, (b) the proportion of double/triple/aromatic bonds, (c) the value of the HOMO-LUMO Gap (gap), and (d) the value of u0, respectively. The vertical axis corresponds to the average test MAE (that is, the smaller, the more accurate).

Under Scenario 1, most of the molecules used for training have a number of atoms ranging from 3 to 15. For molecules with 15 or more atoms, mainly in the test data set, IPS consistently outperforms the other methods. Under Scenario 2, most of the molecules used for training have a proportion of double/triple/aromatic bonds higher than 0.3. Again, on those molecules with proportion less than 0.3, IPS consistently performs better than the others. Similarly in Scenarios 3 and 4, we observe the advantage of IPS for the smaller indicator values corresponding to the test datasets.

Why does the DIRL approach fail? The DIRL approach [8] is a more complicated and modern approach for adapting two datasets from different domains with different distributions, which is known to perform better than the IPS approach on many tasks. However, from our experimental results, it is very surprising that the DIRL approach performs very poorly in the chemical property prediction under the biases. We attribute some of this failure in part to the recent discussion about transferability and discriminability; in their words, while the model achieves high transferability, it fails in discriminability [4]. The DIRL approach finds a space where the molecules from the training set and the target chemical universe are indistinguishable. However, when the information that is useful for discriminating the two domains is also useful for predicting

the chemical property, it is eliminated by the domain-invariant approach, which results in poor discriminability (in other words, prediction power). For example, in Scenario 4, the indicator for introducing the biases and the target chemical property are strongly correlated, as is evident from the definition. Since the other indicators are also very basic chemical properties, it would not be surprising if the information useful for predicting them were also highly related with that for the target chemical properties.

5 Related Work

The existence of experimental biases has been presented in the literature in the field of chemical, physical, biological, and pharmaceutical sciences. For instance, choices of compounds to be investigated are encouraged/discouraged by various physical and chemical properties of compounds, for example, solubility [24], weight [29], toxicity [13], and side effects, or by factors related to the molecular structure such as crystals [17]. In the pharmaceutical domain, drug likeness is an important factor for target selection, as exemplified by the ‘‘Lipinski’s rules of five’’ [22]. Concerns about the cost, availability, experimental methods [37], and research trends [15] can also be sources of bias in the selection. The present study focuses on properties of compounds themselves, but experimental biases in their interactions such as drug-target interactions have also been reported [44,25]. Although the existing studies report negative impacts on the performance of predictive modeling using biased datasets [18,38,3], to the best of our knowledge, there has been no attempt to mitigate the biases to improve the predictive performance.

Recent significant developments in deep neural networks have expanded their scope from vector data to texts and images, and even to graph-structured data. Graph neural networks are actively being studied [12,40] and successfully applied to chemical and physical domains [6,19,36,11,21,42,47]. We used one of the well-known fairly general GNNs [9] in this study, but more modern architectures have been proposed, e.g., one incorporating attention [36] and another with more expressive power [41]. Most of the existing studies assume unbiased datasets, and the present study is the first to address the bias mitigation problem in learning GNNs, except for the one considering classification *on a single large graph* [10], while we consider the classification *of a set of small graphs*.

To mitigate the biases in the experimental datasets, the present study applies two techniques from domain adaptation and causal inference. The problems of learning prediction models, when the distributions of the training dataset and the test dataset are different, are called domain adaptation, covariate shift adaptation [27], or transfer learning [26], and have been a major topic in machine learning. Recently, deep neural networks for domain adaptation based on the idea of domain-invariant representation learning (DIRL) were proposed [8,35]. In this study, we combined DIRL with GNNs, but contrary to our expectations, the approach performed quite poorly. As we discussed in the experimental sec-

tion, some more recent approach balancing transferability and discriminability might offer a solution to this issue [4].

The problem of biased observations is also discussed in the context of causal inference. In this study, we applied the inverse propensity scoring (IPS) method [16], which yields remarkable improvements in prediction performance. IPS is also successfully applied to various applications including recommender systems [32]. The DIRM approach is also proposed in the context of causal inference [33].

6 Conclusion

We tackled the problem of applying machine learning approaches to chemical property prediction from datasets including experimental biases. We introduced bias mitigation methods by combining the recent developments in causal inference, domain adaptation, and graph learning, i.e., the inverse propensity scoring (IPS) and the domain invariant representation learning (DIRL) combined with graph neural networks (GNNs). We simulated four practical biased sampling scenarios on the well-known QM9 dataset. The experimental results confirmed that the IPS approach improved the performance for chemical property prediction with statistical significance, while the DIRM approach was not effective in this domain. Although the domain-invariant approach performed poorly on our settings, our considerations on the failure of DIRM suggest there may be space for improvement, if information for the final predictor can be somehow kept uneliminated by the domain classifier.

Acknowledgments

We are grateful to Yoshihiro Yamanishi, Ichihigaku Takigawa, and Shonosuke Harada for valuable information and discussions.

References

1. Aihara, J.: Reduced HOMO-LUMO gap as an index of kinetic stability for polycyclic aromatic hydrocarbons. *The Journal of Physical Chemistry A* **103**(37), 7487–7495 (1999)
2. Akita, H., Nakago, K., Komatsu, T., Sugawara, Y., Maeda, S.i., Baba, Y., Kashima, H.: Bayesgrad: Explaining predictions of graph convolutional networks. In: *Proceedings of the 25th International Conference on Neural Information Processing (ICONIP)*. pp. 81–92. Springer (2018)
3. Chen, G., Chen, P., Hsieh, C.Y., Lee, C.K., Liao, B., Liao, R., Liu, W., Qiu, J., Sun, Q., Tang, J., et al.: Alchemy: A quantum chemistry dataset for benchmarking ai models. *arXiv preprint arXiv:1906.09427* (2019)
4. Chen, X., Wang, S., Long, M., Wang, J.: Transferability vs. discriminability: Batch spectral penalization for adversarial domain adaptation. In: *Proceedings of the 36th International Conference on Machine Learning (ICML)*. pp. 1081–1090 (2019)

5. De Cao, N., Kipf, T.: Molgan: An implicit generative model for small molecular graphs. In: Proceedings of the ICML 2018 workshop on Theoretical Foundations and Applications of Deep Generative Models (2018)
6. Duvenaud, D.K., Maclaurin, D., Iparraguirre, J., Bombarell, R., Hirzel, T., Aspuru-Guzik, A., Adams, R.P.: Convolutional networks on graphs for learning molecular fingerprints. In: Advances in Neural Information Processing Systems 28. pp. 2224–2232 (2015)
7. Fey, M., Lenssen, J.E.: Fast graph representation learning with PyTorch Geometric. In: Proceedings of the ICLR Workshop on Representation Learning on Graphs and Manifolds (2019)
8. Ganin, Y., Ustinova, E., Ajakan, H., Germain, P., Larochelle, H., Laviolette, F., Marchand, M., Lempitsky, V.: Domain-adversarial training of neural networks. *Journal of Machine Learning Research* **17**(1), 2096–2030 (2016)
9. Gilmer, J., Schoenholz, S.S., Riley, P.F., Vinyals, O., Dahl, G.E.: Neural message passing for quantum chemistry. In: Proceedings of the 34th International Conference on Machine Learning (ICML). pp. 1263–1272 (2017)
10. Guo, R., Li, J., Liu, H.: Learning individual causal effects from networked observational data. In: Proceedings of the 13th International Conference on Web Search and Data Mining (WSDM). pp. 232–240 (2020)
11. Hamilton, W., Ying, Z., Leskovec, J.: Inductive representation learning on large graphs. In: Advances in neural information processing systems. pp. 1024–1034 (2017)
12. Hamilton, W.L., Ying, R., Leskovec, J.: Representation learning on graphs: Methods and applications. *IEEE Data Engineering Bulletin* (2017)
13. Hamm, M.M.: Molecular obesity, potency and other addictions in drug discovery. *Medicinal Chemistry Communication* **2**(5), 349–355 (2011)
14. Harada, S., Akita, H., Tsubaki, M., Baba, Y., Takigawa, I., Yamanishi, Y., Kashima, H.: Dual graph convolutional neural network for predicting chemical networks. *BMC Bioinformatics* **21**, 1–13 (2020)
15. Hattori, K., Wakabayashi, H., Tamaki, K.: Predicting key example compounds in competitors’ patent applications using structural information alone. *Journal of Chemical Information and Modeling* **48**(1), 135–142 (2008)
16. Imbens, G.W., Rubin, D.B.: Causal inference in statistics, social, and biomedical sciences. Cambridge University Press (2015)
17. Jia, X., Lynch, A., Huang, Y., Danielson, M., Langat, I., Milder, A., Ruby, A.E., Wang, H., Friedler, S.A., Norquist, A.J., et al.: Anthropogenic biases in chemical reaction data hinder exploratory inorganic synthesis. *Nature* **573**(7773), 251–255 (2019)
18. Kearnes, S., Goldman, B., Pande, V.: Modeling industrial ADMET data with multitask networks. arXiv preprint arXiv:1606.08793 (2016)
19. Kearnes, S., McCloskey, K., Berndl, M., Pande, V., Riley, P.: Molecular graph convolutions: moving beyond fingerprints. *Journal of Computer-Aided Molecular Design* **30**(8), 595–608 (2016)
20. Kingma, D.P., Ba, J.: Adam: a method for stochastic optimization. *corr abs/1412.6980* (2014) (2014)
21. Li, R., Wang, S., Zhu, F., Huang, J.: Adaptive graph convolutional neural networks. arXiv preprint arXiv:1801.03226 (2018)
22. Lipinski, C.A.: Lead-and drug-like compounds: the rule-of-five revolution. *Drug Discovery Today: Technologies* **1**(4), 337–341 (2004)

23. Liu, Q., Allamanis, M., Brockschmidt, M., Gaunt, A.: Constrained graph variational autoencoders for molecule design. In: *Advances in Neural Information Processing Systems* 31. pp. 7795–7804 (2018)
24. Llinas, A., Burley, J.C., Box, K.J., Glen, R.C., Goodman, J.M.: Diclofenac solubility: independent determination of the intrinsic solubility of three crystal forms. *Journal of Medicinal Chemistry* **50**(5), 979–983 (2007)
25. Mestres, J., Gregori-Puigjane, E., Valverde, S., Sole, R.V.: Data completeness is the Achilles heel of drug-target networks. *Nature Biotechnology* **26**(9), 983–984 (2008)
26. Pan, S.J., Yang, Q.: A survey on transfer learning. *IEEE Transactions on Knowledge and Data Engineering* **22**(10), 1345–1359 (2009)
27. Quionero-Candela, J., Sugiyama, M., Schwaighofer, A., Lawrence, N.D.: *Dataset Shift in Machine Learning*. The MIT Press (2009)
28. Ramakrishnan, R., Dral, P.O., Rupp, M., Von Lilienfeld, O.A.: Quantum chemistry structures and properties of 134 kilo molecules. *Scientific Data* **1**, 140022 (2014)
29. Raymer, B., Bhattacharya, S.K.: Lead-like drugs: A perspective: Miniperspective. *Journal of Medicinal Chemistry* **61**(23), 10375–10384 (2018)
30. Ruddigkeit, L., Van Deursen, R., Blum, L.C., Reymond, J.L.: Enumeration of 166 billion organic small molecules in the chemical universe database gdb-17. *Journal of Chemical Information and Modeling* **52**(11), 2864–2875 (2012)
31. Rupp, M., Tkatchenko, A., Müller, K.R., Von Lilienfeld, O.A.: Fast and accurate modeling of molecular atomization energies with machine learning. *Physical Review Letters* **108**(5), 058301 (2012)
32. Schnabel, T., Swaminathan, A., Singh, A., Chandak, N., Joachims, T.: Recommendations as treatments: Debiasing learning and evaluation. In: *Proceedings of the 33rd International Conference on Machine Learning (ICML)* (2016)
33. Shalit, U., Johansson, F.D., Sontag, D.: Estimating individual treatment effect: generalization bounds and algorithms. In: *Proceedings of the 34th International Conference on Machine Learning (ICML)*. pp. 3076–3085 (2017)
34. Sousa-Silva, C., Petkowski, J.J., Seager, S.: Physical chemistry chemical physics. *Phys. Chem. Chem. Phys.* **21**, 18970–18987 (2019)
35. Tzeng, E., Hoffman, J., Saenko, K., Darrell, T.: Adversarial discriminative domain adaptation. In: *Proceedings of the IEEE Conference on Computer Vision and Pattern Recognition (CVPR)*. pp. 7167–7176 (2017)
36. Veličković, P., Cucurull, G., Casanova, A., Romero, A., Liò, P., Bengio, Y.: Graph attention networks. In: *Proceedings of the Sixth International Conference on Learning Representations (ICLR)* (2018)
37. Walker, R., Bedson, P., Lawn, R., Barwick, V.J., Burke, S., Roper, P.: *Applications of Reference Materials in Analytical Chemistry*. The Royal Society of Chemistry (2001)
38. Wallach, I., Heifets, A.: Most ligand-based classification benchmarks reward memorization rather than generalization. *Journal of Chemical Information and Modeling* **58**(5), 916–932 (2018)
39. Wang, H., Lian, D., Zhang, Y., Qin, L., Lin, X.: Gognn: Graph of graphs neural network for predicting structured entity interactions. In: *Proceedings of the 29th International Joint Conference on Artificial Intelligence (IJCAI)* (2020)
40. Wu, Z., Pan, S., Chen, F., Long, G., Zhang, C., Philip, S.Y.: A comprehensive survey on graph neural networks. *IEEE Transactions on Neural Networks and Learning Systems* (2020)
41. Xu, K., Hu, W., Leskovec, J., Jegelka, S.: How powerful are graph neural networks? In: *Proceedings of the Sixth International Conference on Learning Representations (ICLR)* (2018)

42. Yan, S., Xiong, Y., Lin, D.: Spatial temporal graph convolutional networks for skeleton-based action recognition. arXiv preprint arXiv:1801.07455 (2018)
43. Yao, L., Li, S., Li, Y., Huai, M., Gao, J., Zhang, A.: Representation learning for treatment effect estimation from observational data. In: Bengio, S., Wallach, H., Larochelle, H., Grauman, K., Cesa-Bianchi, N., Garnett, R. (eds.) *Advances in Neural Information Processing Systems* 31, pp. 2633–2643 (2018)
44. Yildirim, M.A., Goh, K.I., Cusick, M.E., Barabási, A.L., Vidal, M.: Drugtarget network. *Nature Biotechnology* **25**(10), 1119–1126 (2007)
45. Ying, Z., Bourgeois, D., You, J., Zitnik, M., Leskovec, J.: Gnnexplainer: Generating explanations for graph neural networks. In: *Advances in Neural Information Processing Systems* 32. pp. 9244–9255 (2019)
46. You, J., Liu, B., Ying, Z., Pande, V., Leskovec, J.: Graph convolutional policy network for goal-directed molecular graph generation. In: *Advances in Neural Information Processing Systems* 31. pp. 6410–6421 (2018)
47. Yu, B., Yin, H., Zhu, Z.: Spatio-temporal graph convolutional networks: A deep learning framework for traffic forecasting. arXiv preprint arXiv:1709.04875 (2017)